Fukushima J. Med. Sci.,
Vol. 55, No. 1, 2009

[Original Article]

SEPARATE DEMONSTRATION OF ARTERIAL- AND VENOUS-PHASE BY 3D-CT ANGIOGRAPHY FOR BRAIN TUMORS USING 64-MULTIDETECTOR ROW CT: 3D-CT ARTERIOGRAPHY AND 3D-CT VENOGRAPHY

HIROMICHI KASUYA[1], MASATO MATSUMOTO[1], RYOJI MUNAKATA[1], HIROYUKI MURAMATSU[1], TSUYOSHI ICHIKAWA[2], TAKU SATO[1], YUJI ENDO[1], JUN SAKUMA[1], KYOUICHI SUZUKI[2], TATSUYA SASAKI[1] and NAMIO KODAMA[1]

[1]*Department of Neurosurgery, Fukushima Medical University; and,* [2]*Department of Neurosurgery, Fukushima Red Cross Hospital, Fukushima, Japan*

(Received November 11, 2008, accepted December 9, 2008)

Abstract: We assessed the usefulness of the separate demonstration of the arterial- and venous phase on 3D-CT angiography (3D-CTA) using a 64-multidetector row CT (MDCT) scanner for the surgery of brain tumors.

Nineteen patients with meningiomas ($n=11$), schwannomas, metastatic brain tumors ($n=2$ each), glioblastoma multiforme, malignant lymphoma, craniopharyngioma, and embryonal carcinoma ($n=1$ each) underwent scanning on a 64-MDCT scanner. After dynamic CT scanning to determine the scan timing for the arterial- and venous-phase, we individually scanned the arterial- and venous phase for 4 sec after injecting a nonionic contrast medium. Using the CT threshold setting and subtraction and cutting techniques, we produced individual 3D-CT images of the arteries, veins, tumors, and bones. The operators subjectively assessed the usefulness of these images in comparison with 3D-CTA.

We separately demonstrated the arterial- and venous phase on 3D-CTA covering the entire head in all 19 cases. The 3D-CT arteriographs, 3D-CT venographs, and the fused 3D-CT images facilitated our understanding of the 3D anatomic relationship among the tumor, arteries, veins, and bony structures. In 14 of 19 cases our method provided the surgically valuable findings; the information on the anatomical relation between tumor and the surrounding arteries and veins (in 13 cases) the identification of anatomical course of the encased vessels (in one), and feeding arteries and draining veins (in one), and discrimination between the venous sinus and tumor (in one).

The anatomical information yielded by our technique makes safer surgery possible. If more detailed information which 3D-CTA cannot provide is required,

粕谷泰道，松本正人，宗像良二，村松広行，市川　剛，佐藤　拓，遠藤雄司，佐久間潤，鈴木恭一，佐々木達也，児玉南海雄
Corresponding author: Hiromichi Kasuya　E-mail: kasuya@fmu.ac.jp
http://fmu.ac.jp/home/lib/F-igaku/　http://www.sasappa.co.jp/online/

our method should be performed.

Key words: 3D-CT arteriography, 3D-CT venography, MDCT, Brain tumor, 3D-CT angiography

INTRODUCTION

3D-CT angiography (3D-CTA) visualizes the anatomical relationships among lesions, surrounding blood vessels, and bones on 3D images. It has been widely used in the diagnosis of central nervous system diseases and surgical simulations[1-6]. 3D-CTA is particularly useful in the diagnosis of patients with cerebrovascular diseases[2-5,7]. However, there have been few reports documenting the value of 3D-CTA in patients with brain tumors[8-10] because information for diagnosis and surgery can be obtained from MRI-and/or catheter cerebral angiography (CCA) studies.

Because knowledge on the 3D anatomy of the tumor and surrounding vessels and bone is necessary for safer surgery, it has been reported 3D-CTA to acquire information of value for preoperative planning[8,10]. However, 3D-CTA does not yield findings on feeding arteries, draining veins, vessels encased by the tumor, and the nature of neighboring vessels. Therefore, we developed a novel technique that facilitates the separate demonstration of the arterial- and venous phase at 3D-CTA in a single procedure[11]. The images provided anatomical details regarding the tumor, arteries, and veins. However, in some instances the entire tumor and/or surrounding structures were not demonstrated because the scan range on the 16-row CT scanner (16-MDCT) was limited to 45 mm.

Recently, a 64-MDCT scanner that features better spatial resolution, a wider-scan range, and shorter data acquisition time than the 16-MDCT scanners has been introduced[12,13]. Using a 64-MDCT we assessed the usefulness of the separate demonstration of the arterial and venous phases on 3D-CTA for preoperative surgical planning in patients with brain tumors.

MATERIALS AND METHODS

The study population consisted of 19 operated patients with pathologically confirmed meningiomas ($n=11$), schwannomas, metastatic brain tumors ($n=2$ each), glioblastoma multiforme, malignant lymphoma, craniopharyngioma, and embryonal carcinoma ($n=1$ each) (Table 1). The 19 patients was already performed 3D-CTA, but we added the scanning for the separate demonstration of the arterial and venous phases on 3D-CTA because we needed the more detailed information such as anatomical relation between arteries and veins, the vessels encased by tumor and the identification of arteries or veins.

Table 1. Clinical information on 19 patients with brain tumors

Case No.	Age/ Sex	Diagnosis	PTA(s)	PTV(s)	Arterial phase scan (s)	Venous phase scan (s)	Pulse rate(1) /min	Pulse rate(2) /min	Surgeon	Useful findings
1	80/F	Falx Meningioma	17	24	14-18	24-28	60	59	M.M.	b
2	69/F	Falx Meningioma	17	21	15-19*	22-26*	83	75	M.M.	b
3	49/M	Falx Meningioma	17	21	14-18	21-25	80	78	N.K	b
4	70/F	Multiple Meningioma	15	20	12-16	20-24	77	75	T.S.	b
5	49/F	Multiple Meningioma	16	21	13-17	21-25	63	64	M.M.	a, b
6	55/F	Olfactory Meningioma	18	25	15-19	25-29	76	77	M.M.	b, d
7	53/F	Tuberculum Sellae Meningioma	17	22	14-18	22-26	62	63	T.S.	none
8	26/F	Parasagittal Meningioma	15	19	12-16	19-23	83	81	T.S.	c
9	74/M	Sphenoid Ridge Meningioma	18	25	15-19	25-29	78	78	N.K.	b
10	34/M	Middle Fossa Meningioma	14	21	11-15	21-25	54	63	N.K.	b
11	52/F	Foramen Magnum Meningioma	19	24	16-20	24-28	51	51	N.K.	b
12	57/M	Trigeminal Schwannoma	18	24	15-19	24-28	62	64	M.M.	b
13	53/F	Trigeminal Schwannoma	19	25	16-20	25-29	57	57	N.K.	b
14	57/M	Metastatic Brain Tumor	19	25	16-20	25-29	61	63	M.M.	none
15	56/F	Metastatic Brain Tumor	17	23	14-18	23-27	64	63	N.K	none
16	68/F	Glioblastoma Multiforme	14	19	11-15	19-23	64	64	M.M.	none
17	72/F	Malignant Lymphoma	18	26	15-19	26-30	63	62	N.K.	b
18	41/M	Craniopharyngioma	16	22	13-17	22-26	71	73	N.K.	none
19	32/M	Embryonal Carcinoma	15	23	12-16	23-28	65	64	N.K.	b

PTA: peak time for the internal carotid artery, PTV: peak time for the sigmoid sinus, Pulse rate (1): pulse rate during dynamic CT scanning, Pulse rate (2): pulse rate just before the scanning of arterial-phase, *: the scan timings of arterial and venous phase were delayed for 1 second, respectively. s: second, min: minute, three findings: a, identification of anatomical course of the encased vessels: b, anatomical relation between tumor and the surrounding arteries and veins: c, discrimination between venous sinus and tumor: none, no significant useful findings: d, feeding arteries and draining veins.

We used a 64-MDCT scanner (Aquilion, Toshiba Corporation, Tokyo) with a tiltable gantry. First, we obtained scout views to determine the scan range for dynamic CT scanning. To reduce radiation exposure to the orbits, the scanning range was set from the orbitomeatal (OM) line 10 mm above and parallel with the OM line ; it facilitated scanning of the internal carotid artery (ICA) in the cavernous sinus and sigmoid sinus (SS). An 18-gauge plastic intravenous catheter was placed in an antecubital vein and connected to a dual-head power injector. Dynamic CT scanning was started 5 sec after the injection of nonionic contrast material (Iopamiron® ; 370 mg/dl, Schering, Osaka, Japan) at a rate of 6 ml/sec for 3 sec (total volume 18 ml) followed by a chaser bolus-injection of saline (total volume 12 ml, delivered at 6 ml/sec for 2 sec). A dynamic CT scan (four 4-mm-thick slices) was obtained every 0.5 sec for a total of 25 sec. The X-ray tube voltage/current was 80 kV/60 mA. We produced time-density curves by setting the regions of interest at the ICA in the cavernous- and sigmoid sinus (Fig. 1A, B).

Based on the dynamic CT results we determined the optimal scan timing for the arterial- and venous phase. The arterial phase was scanned from 3 sec before the peak of the time density curve of the ICA to 1 sec after the peak. The venous phase was scanned from the peak time of the SS to 4 sec after the peak (Fig. 1B). After approximately 10 min, the arterial- and venous phases were scanned individually after contrast injection (Fig. 2). We interposed the 10-min interval because the concentration of contrast medium injected for dynamic CT scanning affects the image quality of arterial- and venous-phase 3D-CTA images. The patient's heart

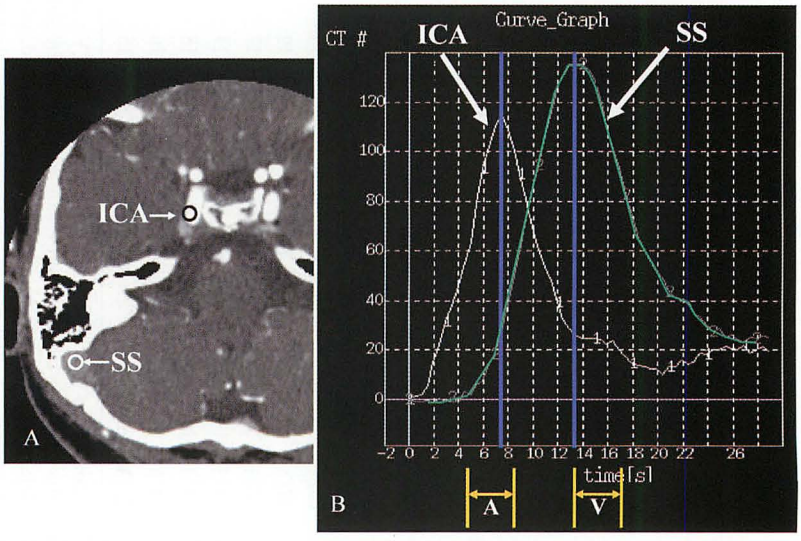

Fig. 1. A : Regions of interest at the ICA in the cavernous sinus and the SS are set on the axial image. ICA=internal carotid artery, SS=sigmoid sinus. B : Scan timing for the arterial and venous phases was determined by the time density curves of the ICA and SS. A=arterial-phase scan, V=venous-phase scan

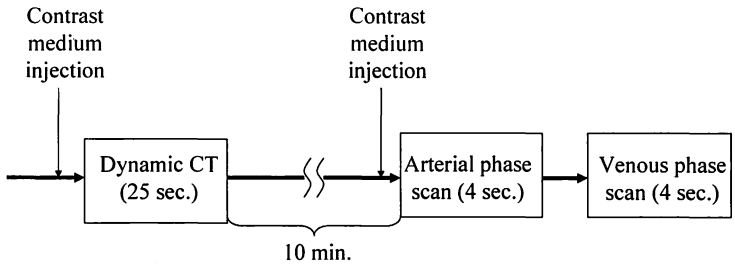

Fig. 2. Our scanning protocol. The acquisition of arterial- and venous-phase scans was followed by dynamic CT scanning. The interval between dynamic CT- and arterial-phase scanning was approximately 10 min. sec=second, min=minute

rate was monitored throughout the examination. When there was a difference of more than 8 beats between the heart rate during the dynamic CT scan and the heart rate just prior to arterial-phase scanning, the scan timing for the arterial and venous phases was adjusted.

The scan parameters were as follows: 135 kV, 260 mA, helical pitch, 41 ; 0.5 sec per tube rotation ; tube speed, 36 mm/sec ; scan range, 120 mm. Using a dual-head power injector, we delivered a bolus injection of contrast medium at a rate of 6 ml/sec for 5 sec (total 30 ml) ; this was followed by an 18-ml saline chaser bolus administered at a rate of 6 ml/sec.

The acquired data were reconstructed at 0.3-mm slice thickness and transferred to a workstation (ZIO M900 QUADRA, Ziosoft Inc., Tokyo) connected on-line to the MDCT scanner. First, we produced arterial- and venous-phase 3D-CTA images with a volume-rendering technique. The lower threshold of 110-160 Hounsfield units (HU) allowed the extraction of arterial-phase 3D-CTA images without veins and of venous-phase 3D-CTA images without arteries. Next, we created bone images from the venous-phase 3D-CTA images at a 260-450 HU threshold. Using the dilate function of the workstation, we increased the thickness of the bone images by 7 pixel layers (Fig. 3D), because there was a difference of 7 pixels between the bone images at a 260-450 HU threshold and the original bone images. The dilated image was then subtracted from the arterial-phase 3D-CTA image, this yielded 3D-CT images of the arteries demonstrated on arterial-phase scans (Fig. 3A). Similarly, the dilated bone image was subtracted from the venous-phase 3D-CTA image, yielding 3D-CT images of the veins demonstrated at the venous-phase (Fig. 3B). Lastly, the tumor was extracted from the 3D-CT images of arteries or veins by using a cutting method (Fig. 3C). In cases where the tumor was markedly or moderately enhanced, it was extracted at a lower threshold (80-120 HU). In the patient with a non-enhanced craniopharyngioma (case 18, Table 1), the tumor was extracted at a lower threshold (0-10 HU). To identify the arteries, veins, bone, and tumor, they were colored red, blue, white, and green, respectively. Using these 3D-CT images we prepared combined images, i.e. 3D-CT arteriography (3D-CT image of arteries and bone), 3D-CT venography (3D-CT image of veins and bone), and fused 3D-CT

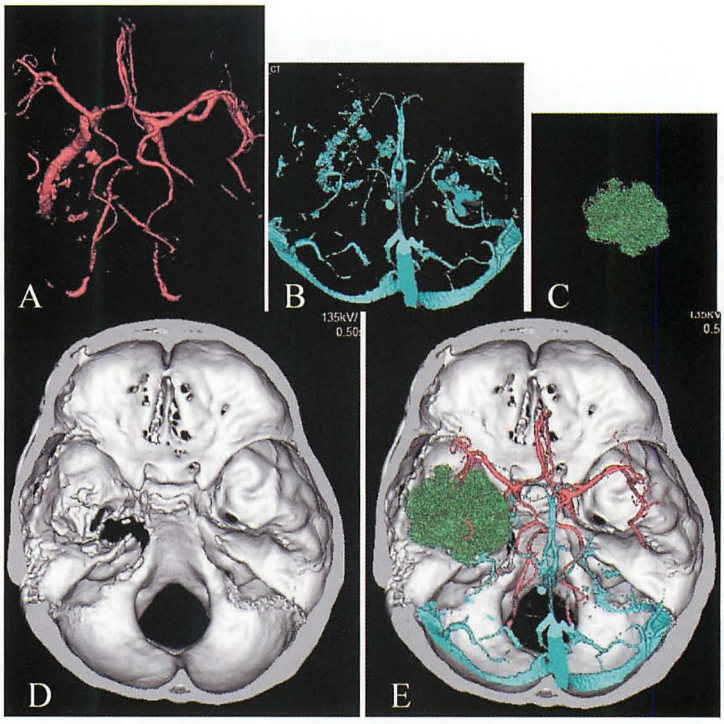

Fig. 3. 3D images generated with the 64-detector MDCT scanner. A: Image of arteries. B: Image of veins. C: Image of the tumor. D: Image of bone. E: Fused 3D-CT image, superior view, showing the anatomical relationship among arteries, veins, bone, and tumor.

images of the arteries, veins, bone, and tumor (Fig. 3E). To assess the vessels involved by the tumor, semitransparent images of the tumor were created. Tumors that were not demarcated were not extracted because it was difficult to delineate the tumor margin.

Three experienced neurosurgeons (N.K., T.S., M.M.) who performed the operation reviewed the images after the operation and assessed what findings of our method were useful for the surgery in comparison with 3D-CTA. They were asked to subjectively evaluate our method concerning the following findings such as identification of anatomical course of the encased vessels, anatomical relation between tumor and the surrounding arteries and veins, and discrimination between venous sinus and tumor.

Informed consent was obtained from the patients before the imaging.

RESULTS

The 64-MDCT scanner consistently provided arterial- and venous-phase 3D-CTA of the entire head. In all 19 cases, by setting the CT threshold at 110-160 HU, we were able to demonstrate arterial- and venous-phase 3D-CTA images separate-

ly. Of the 19 tumors, 18 were successfully extracted from the 3D-CT venographs. We were unable to extract the glioblastoma multiforme (case 16, Table 1) because the tumor border was obscure.

Our technique yielded 3D-CT arteriography-, 3D-CT venography-, and fused 3D-CT images that made possible an understanding of the anatomic 3D relationship among the arteries, veins, bony structures, and tumors. These images provided useful information that could not be obtained on 3D-CTA on the feeding arteries, draining veins, the vessels involved by the tumor, sinus invasion by the tumor, and made possible the identification of arteries or veins surrounding the tumor. According to the assessment of the three operators, the usefulness of our method was indicated in 14 of the 19 cases. The information on the anatomical relation between tumor and the surrounding arteries and veins was useful in 13 of the 14 cases and on feeding arteries and draining veins was in one, the identification of anatomical course of the encased vessels was in one, and the discrimination between the venous sinus and tumor was in one. In 5 cases, our method did not provide significant useful findings for the operator.

In case 2, an 80-year-old woman with a falx meningioma, there was a difference in 8 beats between the heart rate at dynamic CT- and just before arterial-phase scanning. To adjust the scan timing, we delayed for 1 sec the acquisition of arterial- and venous-phase scans. This allowed for the successful creation of arterial- and venous phase 3D-CTA images. Other than some reports of a warming sensation throughout body, we encountered no adverse events in this series.

In 2 of the 19 cases (cases 6 and 10), we performed CCA to embolized the feeding arteries. In case 10, we embolized the middle meningeal artery feeding the tumor. In case 6, we did not perform embolization because the feeding arteries derived from ethmoidal arteries of the ophthalmic artery.

Representative Cases

Case 5. This 49-year-old woman with multiple atypical meningiomas was admitted to our hospital for resection of a recurred tumor in the middle fossa. T1-weighted gadolinium-enhanced MRI showed an enhanced mass in the right middle fossa (Fig. 4A). Although 3D-CTA demonstrated the tumor and surrounding vessels (Fig. 4B), it did not provide information on involved vessels and whether these were arteries or veins. Fused 3D-CT images of the arteries, veins, and the tumor made it possible to identify the arteries and veins on the surface of the tumor (Fig. 4C). On these images the tumor was semitransparent and we were able to understand the anatomical course of the sphenoidal (M1)- and insular segment (M2) of the right middle cerebral artery (MCA) involved by the tumor (Fig. 4D). These findings were consistent with surgical observations. Based on this information, we were able to remove the tumor without any damage to the encased M1 and M2 segments.

Case 6. This 55-year-old woman was admitted to our hospital with visual impairment and a disturbance of her sense of smell. Gadolinium-enhanced T1-

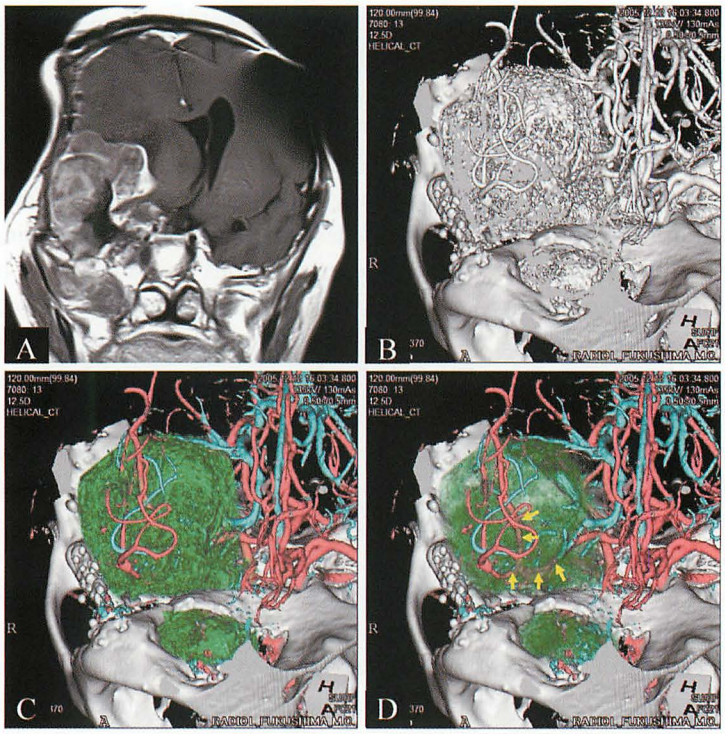

Fig. 4. Case 5—A 49-year-old woman with multiple meningiomas. A : Gadolinium-enhanced T1-weighted MRI showed an enhanced mass in the right middle fossa. B : 3D-CTA, anterosuperior view, demonstrated the tumor in the middle fossa and surrounding vessels. C : Fused 3D-CT image of arteries, veins, and tumor, anterosuperior view, showed the anatomic relationship among arteries, veins, and tumor. D : On the fused 3D-CT image the tumor is semitransparent. This makes it possible to discern the anatomic course of the M1 and M2 (arrows) segment of the right MCA involved by the tumor. M1=sphenoidal segment, M2=insular segment, MCA=middle cerebral artery

Fig. 5. Case 6—A 55-year-old woman with olfactory meningioma. A : Gadolinium-enhanced T1-weighted MRI demonstrated an enhanced mass. B : 3D-CTA, superior view, showed the tumor and surrounding vessels. C : Fused 3D-CT image (superior view) showed the anatomic relationship among the tumor, arteries, and veins. D : Fused 3D-CT image, right lateral view. The semitransparency of the tumor made it possible to identify the draining veins (arrows). E : The 3D-CT arteriography demonstrated the feeding arteries (arrow) exhibiting radiated features, the so-called "sun-burst appearance", at the center of the tumor. F, G : Compared to the fused 3D-CT- and the 3D-CTA images, right internal carotid artery angiograms obtained during the arterial (F) and venous (G) phase, right lateral view, did not clearly visualize the feeding arteries and draining veins.

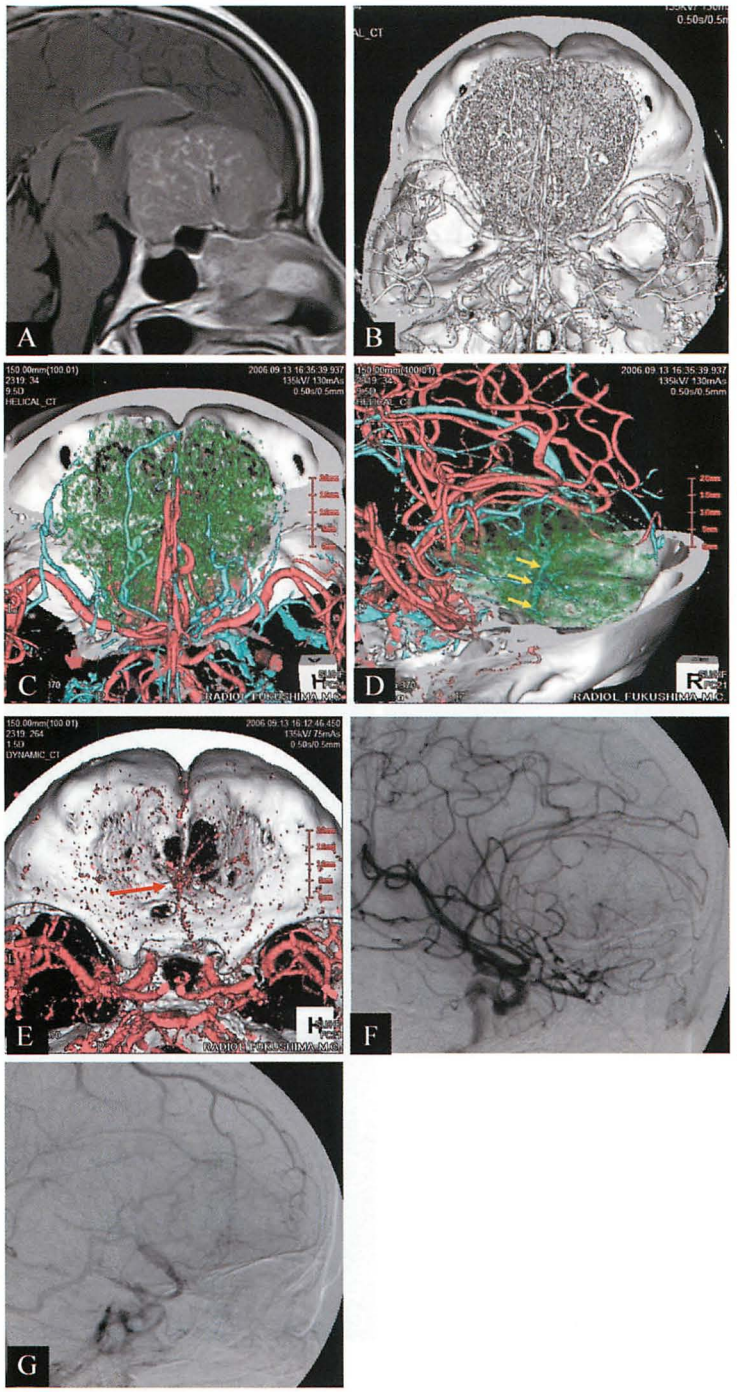
A
B
C
D
E
F
G

weighted MRI demonstrated a mass with a flow void in the anterior fossa (Fig. 5A), pathologically diagnosed as olfactory groove meningioma. Although 3D-CTA visualized the tumor and surrounding vessels, it did not help to identify arteries and veins (Fig. 5B). Fused 3D-CT images facilitated understanding of the anatomic relationship among the tumor, arteries, and veins on the surface of the tumor (Fig. 5C). Moreover, as the tumor was semitransparent, the draining veins in the tumor could be identified (Fig. 5D). The feeding arteries arising at the center of the tumor were visualized on 3D-CT arteriography (Fig. 5E). Although we performed CCA to embolize the feeders from the external carotid artery, we did not follow through because the tumor was supplied from the ophthalmic artery. Compared to CCA (Fig. 5F, G), the 3D-CT images clearly demonstrated the feeding arteries and draining veins. We coagulated the feeding arteries during the early stage of the operation, thereby minimizing bleeding from the tumor.

Case 8. This 26-year-old woman suffered from left hemiparesis. Gadolinium-enhanced T1-weighted MRI demonstrated an enhanced mass attached to the superior sagittal sinus (SSS) (Fig. 6A), pathologically diagnosed as parasagittal meningioma. Although 3D-CTA did not yield information on the patency of the SSS (Fig. 6B), 3D-CT images of the veins indicated that it was patent. Fused 3D-CT images

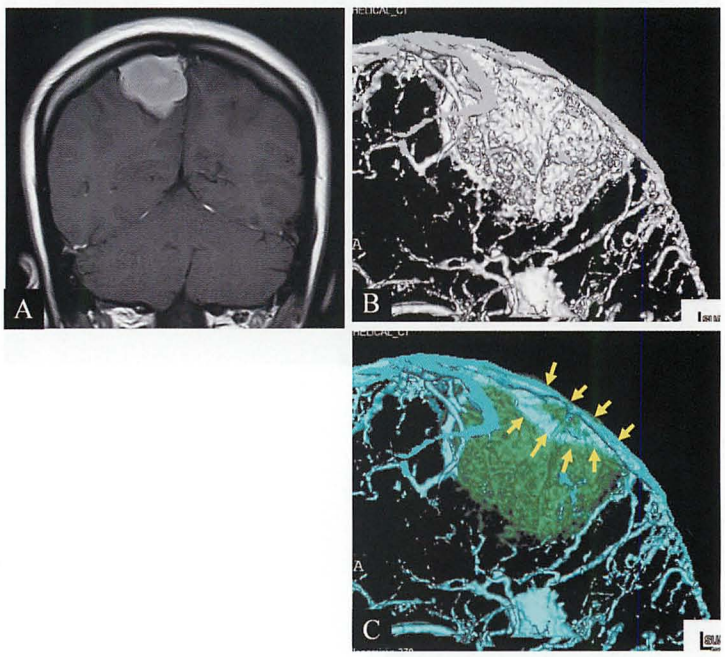

Fig. 6. Case 8—A 26-year-old woman with parasagittal meningioma. A: Gadolinium-enhanced T1-weighted MRI demonstrated a homogeneously enhanced mass which were attached to the superior sagittal sinus (SSS). B: 3D-CTA, right lateral view, did not yield information on the patency of the SSS. C: Fused 3D-CT image of veins and the tumor showing a fenestrated and stenotic SSS (arrows).

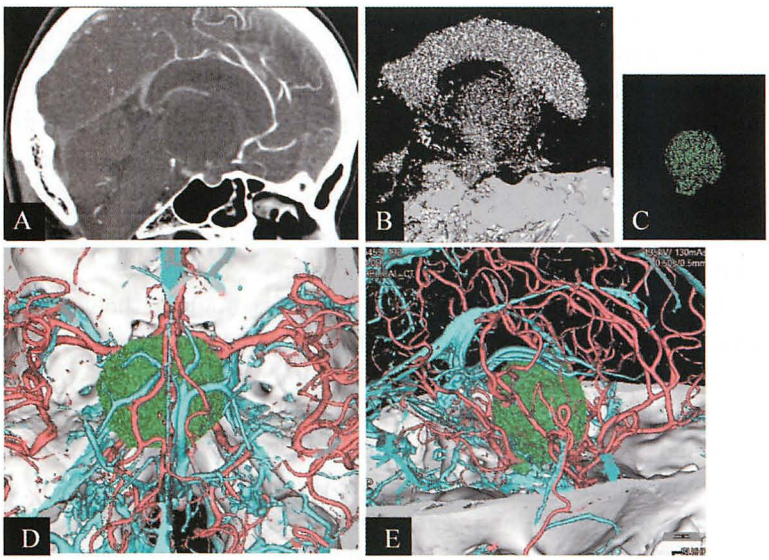

Fig. 7. Case 18—A 41-year-old man with craniopharyngioma. A: Contrast-enhanced CT demonstrated an unenhanced cystic mass in the suprasellar region. B: 3D-CT image, right lateral view, of the lateral ventricle and cyst. Extraction was at a 0-10 HU threshold. C: 3D-CT image of the tumor, right lateral view, extracted by using the cutting method and the color green for identification. D, E: Fused images, superior (D) and right lateral view (E), demonstrated the anatomical relationship among the tumor, displaced arteries, and veins.

revealed fenestration and stenosis of the SSS (Fig. 6C). With this information we were able to ascertain preoperatively the anatomical relationship between the SSS and the tumor. This prevented operative injury of the SSS and facilitated total tumor removal. The patency of the SSS was confirmed at surgery.

Case 18. This 41-year-old man was admitted complaining of visual disturbance. Contrast-enhanced CT demonstrated an unenhanced cystic mass in the suprasellar region (Fig. 7A), pathologically diagnosed as craniopharyngioma. First, we extracted the lateral ventricle and cyst at an HU threshold of 0-10 (Fig. 7B). Next, the green-colored tumor was extracted by using the cutting method (Fig. 7C). Fused 3D-CT images provided information on the anatomical relationship between the tumor and the displaced arteries and veins (Fig. 7D, E).

DISCUSSION

Although the utility of 3D-CTA in patients with cerebrovascular diseases has been documented[1-7], there are few reports on its usefulness in patients with brain tumors[8-10]. One reason why 3D-CTA has been used as a supplemental rather than an essential tool for the evaluation of brain tumors may be that it cannot demonstrate arteries and veins separately. Using a 16-MDCT scanner we previously reported a method that demonstrates separately the arterial- and venous-phase on

3D-CTA[11], however, the tumors larger than 45 mm were not demonstrated. The new 64-MDCT scanner[12,13], opened a larger scan range of 120 mm and is 4 times faster than the 16-MDCT scanner. This facilitated the separate demonstration of the arterial-and venous phase on 3D-CTA of the entire head. Although arteries and veins can be identified on 3D-CTA based on anatomical knowledge, their correct identification depends on the experience and subjective judgment of the viewer and misinterpretation cannot be ruled out. Our method makes possible the unequivocal anatomic differentiation between arteries and veins.

In 18 of 19 cases, the tumors were stained more strongly in the venous—than the arterial phase ; therefore, we extracted the tumors from 3D-CT images of the veins. Even in the patient with a non-enhanced craniopharyngioma (case 18) a 3D-CT image of the tumor could be created using a CT threshold of 0-10 HU. As 3D-CT arteriography and -venography can be combined with the tumor image, information can be gleaned on the 3D relationship among the arteries, veins, tumor, and bone.

To separate the arterial- and venous phase on 3D-CTA, the scan timing of the arterial- and venous phase should be based on time-density curve data acquired from dynamic CT scans. As the arrival time of the injected contrast medium at the ICA depends on the heart rate[6], our method requires that the heart rate during dynamic CT-be equal to the rate during arterial- and venous phase scanning. When there is a difference in 8 beats, there is a time difference in 1 sec between the arrival of the medium at the intracranial ICA[6]. In such cases, the scan timing of the arterial- and venous phase must be corrected to compensate for this difference. In one of 19 cases (case 2), we made this correction and succeeded in developing arterial- and venous phase 3D-CTA images.

Information on the vascular supply to the tumor is important to minimize blood loss during tumor resection. In the patient with meningioma (case 6), 3D-CT arteriography demonstrated feeding arteries that were not clearly visualized on CCA images. The radiated nature of the feeding arteries shown on 3D-CT arteriography may reflect the sun-burst appearance. The 3D features of the feeding arteries may be a characteristic 3D-CT arteriography finding as the CCA finding in cases with meningioma[14].

Moreover, 3D information on encased vessels, especially arteries, is critical for a safer surgical procedure. The semitransparency of the tumor made it possible to evaluate the anatomical course of arteries encased within the tumor. This technique is valuable for preoperative evaluation of the tumor.

When the tumor is enhanced as intensely as the dural sinus, 3D-CTA fails to demonstrate tumor invasion to the dural sinus because it is impossible to visualize infiltration at any window level. Our method makes it possible to differentiate the tumor from the dural sinus ; this allows evaluation of the degree of dural sinus stenosis. However, to differentiate unequivocally between the tumor and the dural sinus, in addition to arterial- and venous phase scanning, a method for tumor-phase scanning is needed.

The findings on the differentiation and/or anatomical course of the vessels which are adjacented to tumors or encased by tumors are important for the operators because the information makes the surgical approach and resection of the tumors safer. This study indicated the usefulness of our technique for the surgery, however, our technique may not be applied for all patients with tumors because the patients suffer from the additional radiation exposure. We believe that our method should be performed in the patients who the information on the 3D-CTA is not sufficient for the operation.

MR angiography (MRA) and MR venography (MRV) facilitate assessment of the arteries and veins. If MRA and MRV images are fused and displayed on 3D-images, the anatomical relation between arteries and veins can be examined. Compared with our method, however, MRA and MRV have relative disadvantages because they do not provide information on bony structures and calcifications; this information is important for surgery. MRA involves a variety of potential artifacts and may result in misinterpretation[15-18]. The susceptibility gradient of the sphenoidal- and ethmoidal sinuses and the turbulent or slow flow within vessels result in signal loss and misdiagnosis[16]. Ayanzen *et al.*[19]. reported that transverse flow-gaps were observed in as many as 31% of patients with normal MRI findings. These flow gaps are mainly related to artifact from slow intravascular blood flow, in-plane flow, and complex flow patterns. The observation of such flow gaps may raise diagnostic difficulties when dural sinus stenosis or occlusion is suspected[20]. Moreover, MRA and MRV are not tolerated by patients with pacemakers or claustrophobia[21,22] and may be susceptible to degradation due to patient motion. On the other hand, our technique is a reliable method to depict the venous structures because it does not involve in-plane saturation. Miki *et al.*[9] compared MDCT- and MR images in the evaluation of pituitary macroadenomas with regard to tumor margin clarity, the identification of the normal pituitary gland and of erosion or destruction of the sellar floor. They reported that MDCT was superior to MRI for assessing lateral tumor margins and the sellar floor at the sphenoid sinus. Although we have no experience with pituitary adenoma patients, we postulate that our method offers useful preoperative information in these patients as well.

Although the features of the vasculature can be visualized on 3D-CTA, it does not yield functional findings. Our method does not provide information regarding perfusion such as the venous circulation in veins or sinuses invaded by the tumor and evaluation of the collateral flow is also difficult. Therefore, CCA remains a useful and necessary technique. Since we delivered the contrast medium as a single bolus injection, the images we obtained may display dynamic information. The visualization of arteries on 3D-CT venography is indicative of a delay in the arterial flow and prolongation in the cerebral circulation. On the other hand, the visualization of veins on 3D-CT arteriography makes it necessary to rule out the presence of an arteriovenous shunt such as an arteriovenous malformation, an arteriovenous fistula, or a malignant tumor with an arteriovenous shunt. In case 16, a patient with

glioblastoma multiforme, the visualization of abnormal vessels in the arterial phase may indicate the existence of arteriovenous shunts, suggesting that tumors harboring abnormal vessels with an arterial component may be malignant[23].

Compared to CCA, our method is less invasive, less expensive and the time required for the acquisition of images is shorter. CCA carries the risk for stroke and limb ischemia[24-26].As it was possible to proceed to surgery in 17 of our 19 cases without subjecting the patients to CCA, we suggest that use of our method makes it possible to operate many brain tumors.

In terms of disadvantages, our procedure requires the acquisition of dynamic CT scans before arterial- and venous-phase scanning. Therefore, patients are subjected to 3 scans with relatively high radiation exposure. To reduce the radiation dose, we performed dynamic CT with a tube voltage/current of 80 kV/60 mA. The estimated radiation dose was approximately 120 mGy. Since the tube voltage/current at scanning of the arterial- and venous phase was 135 kV/260 mA, the estimated radiation dose was approximately 220 mGy, resulting in a total radiation dose of 360 mGy. The radiation dose of perfusion CT is reported to be 700-1,400 mGy[27]. Imanishi *et al.*[28] reported 3 patients who manifested transient bandage-shaped hair loss after perfusion CT with CCA or interventional procedures. Their 3 patients underwent 2 angiographic studies of the head and more than 2 perfusion CT studies within 15 days. The estimated radiation dose to the skin exceeded 3-5 Gy. We must remember that the cumulative or multiplier effect of radiation exposure from multiple diagnostic techniques may result in hair loss and other complications.

We delivered a bolus contrast infusion at the rate of 6 ml/sec ; this is twice the speed of injection used at conventional 3D-CTA. Toyota *et al.*[29] encountered no extravasation of contrast medium delivered at 9 ml/sec nor any other complications. Others who reported contrast infusion rates of 7-10 ml/sec did not discuss complications attributable to the high speed of injection[30-32]. Although we encountered no complications at an infusion rate of 6 ml/sec, special care must be taken when our method is performed on the elderly patients or patients with heart disease.

CONCLUSIONS

The 64-MDCT scanner makes it possible to create whole-head 3D-CT images of the arteries, veins, tumors, and bones. Fused 3D-CT images provided information on the anatomic relationship among the tumor, arteries, veins, and bony structures. They made it possible to assess feeding arteries, draining veins, the patency of the dural sinus invaded by the tumor, encased vessels, and to distinguish between arteries and veins.

Our method is highly useful at preoperative study because it yields findings indispensable for a safer surgical approach. If the information on the 3D-CTA is not sufficient and the more detailed and valuable findings are required, our technique

should be applied.

REFERENCES

1. Aoki S, Sasaki Y, Machida T, Ohkubo T, Minami M, Sasaki Y. Cerebral aneurysms: detection and delineation using 3D-CT angiography. AJNR Am J Neuroradiol, **13**: 1115-1120, 1992.
2. Anderson GB, Findlay JB, Steinke DE, Ashforth R. Experience with computed tomographic angiography for the detection of intracranial aneurysms in the setting of acute subarachnoid hemorrhage. Neurosurgery, **41**: 522-528, 1997.
3. Brandt T, Knauth M, Wildermuch S, Winter R, von Kummer R, Sartor K, Hacke W. CT angiography and Doppler sonography for emergency assessment in acute basilar artery ischemia. Stroke, **30**: 606-612, 1999.
4. Harbaugh RE, Schlusselberg DS, Jeffery R, Hayden S, Cromwell LD, Pluta D, Robert A. Three-dimensional computed tomographic angiography in the preoperative evaluation of cerebrovascular lesions. Neurosurgery, **36**: 320-327, 1995.
5. Matsumoto M, Sato M, Nakano M, Endo Y, Watanabe Y, Sasaki T, Suzuki K, Kodama N. Three-dimensional computerized tomography angiography-guided surgery of acutely ruptured cerebral aneurysms. J Neurosurg, **94**: 718-727, 2001.
6. Nakano M, EndoY, Kobayashi T. [Study on the appropriate scan delay time on helical CT scans] Progress in CI, **20**: 173, 1997 (Abstract) (Jpn).
7. Wintermark M, Uske A, Chalaron M, Regli L, Maeder P, Meuli R, Schnyder P, Binaghi S. Multislice computerized tomography angiography in the evaluation of intracranial aneurysms: A comparison with intraarterial digital subtraction angiography. J Neurosurg, **98**: 828-836, 2003.
8. Clifford JE, Michael HL, Stephen BT, Gilberto GR. Cerebral CT venography in surgical planning for a tentorial meningioma. J Comput Assist Tomogr, **22**: 530-532, 1998.
9. Miki Y, Kanagaki M, Takahashi JA, Ishizu K, Nakagawa M, Yamamoto A, Fushimi Y, Okada T, Mikuni N, Kikuta K, Hashimoto N, Togashi K. Evaluation of pituitary macroadenomas with multidetector-row CT (MDCT): Comparison with MR imaging. Neuroradiology, **49**: 327-333, 2007.
10. Tsuchiya K, Hachiya J, Mizutani Y, Yoshino A. Three-dimensional helical CT angiography of skull base meningiomas. AJNR Am J Neuroradiol, **17**: 933-936, 1996.
11. Matsumoto M, Kodama N, Sakuma J, Sato S, Oinuma M, Konno Y, Suzuki K, Sasaki T, Suzuki K, Katakura T, Shishido F. 3D-CT arteriography and 3D-CT venography. The separate demonstration of arterial-phase and venous-phase on 3D-CT angiography in a single procedure. AJNR Am J Neuroradiol, **26**: 635-641, 2005.
12. Agid A, Lee SK, Willinsky RA, Farb RI, terBrugge KG. Acute subarachnoid hemorrhage: Using 64-slice multidetector CT angiography to "triage" patients' treatment. Neuroradiology, **48**: 787-794, 2006.
13. Lubicz B, Levivier M, Francois O, Thoma P, Sadeghi N, Collignon L, Baleriaux D. Sixty-four-row multisection CT angiography for detection and evaluation of ruptured intracranial aneurysms: Interobserver and intertechnique reproducibility. AJNR Am J Neuroradiol, **28**: 1949-1955, 2007.
14. Krayenbuhl H, Yasargil MG (ed). Cerebral Angiography. Georg Thieme Verlag, New York, 440-452, 1982.
15. Atlas SW. MR angiography in neurologic disease. Radiology, **193**: 1-16,1994.
16. Heiserman JE, Drayer BP, Keller PJ, Fran EK. Intracranial vascular stenosis and occlusion: Evaluation with three-dimensional time-of-flight MR angiography. Radiology, **185**: 667-673, 1992.
17. Okamoto K, Ito J, Furusawa T, Sakai K, Tokiguchi S. "Pseudoocclusion" of the

internal carotid artery: A pitfall on intracranial MRA. J Comput Assist Tomogr, **21**: 831-833, 1997.
18. Tsuruda J, Saloner D, Norman D. Artifacts associated with MR neuroangiography. AJNR Am J Neuroradiol, **13**: 1411-1422, 1992.
19. Ayanzen RH, Bird CR, Keller PJ, McCully FJ, Theobald MR, Heiserman JE. Cerebral MR venography: Normal anatomy and potential diagnostic pitfalls. AJNR Am J Neuroradiol, **21**: 74-78, 2000.
20. Lewin JS, Masryk TJ, Smith AS, Ruggieri PM, Ross JS. Time-of-flight intracranial MR venography: Evaluation of the sequential oblique section technique. AJNR Am J Neuroradiol, **15**: 1657-1664, 1994.
21. Dewey M, Schink T, Dewey CF. Claustrophobia during magnetic resonance imaging: Cohort study in over 55,000 patients. J Magn Reson Imaging, **26**: 1322-1327, 2007.
22. Eshed I, Althoff CE, Hamm B, Hermann KG. Claustrophobia and premature termination of magnetic resonance imaging examinations. J Magn Reson Imaging, **26**: 401-404, 2007.
23. Krayenbuhl H, Yasargil MG (ed). Cerebral Angiography. Georg Thieme Verlag, New York, pp 410-417, 1982.
24. Burows PF, Robertson RL. Barnes PD. Angiography and the evaluation of cerebrovascular disease in childhood. Neuroimaging Clin N Am, **6**: 561-588, 1996.
25. Heiserman JE, Dean BL, Hodak JA, Flom RA, Bird CR, Drayer BP, Fram EK. Neurologic complications of cerebral angiography. AJNR Am J Neuroradiol, **15**: 1401-1407, 1994.
26. Martin B, Martin K, Ralph B, Monika W, Erich H, Laszio S. Silent embolism in diagnostic cerebral angiography and neurointerventional procedures: A prospective study. Lancet, **354**: 1594-1597, 1999.
27. Hirata M, Sugawara Y, Fukutomi Y, Oomoto K, Murase K, Miki H, Mochizuki T. Measurement of radiation dose in cerebral perfusion study. Radiat Med, **23**: 97-103, 2005.
28. Imanishi Y, Fukui A, Niimi H, Itoh D, Nozaki K, Nakaji S, Ishizuka K, Tabata H, Furuya Y, Uzura M, Takahama H, Hashizume S, Arima S, Nkajima Y. Radiation-induced hair loss as a radiation damage only occurring in patients who had the combination of MDCT and DSA. Neuroradiology, **49**: 327-333, 2007.
29. Toyota S, Iwaisako K, Takimoto H, Yoshimine T. Intravenous 3D digital subtraction angiography in the diagnosis of unruptured intracranial aneurysms. AJNR Am J Neuroradiol, **29**: 107-109, 2008.
30. Furukawa M, Kashiwagi S, Matsunaga N, Suzuki M, Kishimoto K, Shirao S. Evaluation of cerebral perfusion parameters measured by perfusion CT in chronic cerebral ischemia: Comparison with Xenon CT. J Comput Assist Tomogr, **26**: 272-278, 2002.
31. Reichenback JR, Rother J, Jonetz-Mentzel L, Herzau M, Fiala A, Weiller C, Kaiser WA. Acute stroke evaluated by time-to-peak mapping during initial and early follow-up perfusion CT studies. AJNR Am J Neuroradiol, **20**: 1842-1850, 1999.
32. Shaefer PW, Roccatagagliata L, Ledezma C, Hoh B, Schwamm LH, Koroshetz W, Gonzalez RG, Lev MH. First-pass quantitative CT perfusion identifies thresholds for salvageable penumbra in acute stroke patients treated with intra-arterial therapy. AJNR Am J Neuroradiol, **27**: 20-25, 2006.